Giant Magnetoresistance Phenomenon in Manganates

C. N. R. Rao*

Abstract: The discovery of giant magnetoresistance (GMR) in rare earth manganates of the general formula $Ln_{1-x}A_xMnO_3$ (Ln = rare earth, A = divalent cation) has aroused much interest not only because of its technological implications, but also due to the fascinating features and mechanism of the phenomemon in these oxides. GMR is observed in these manganates when they become ferromagnetic and transform from an insulating state to a metallic state close to the Curie temperature. The essential features of magnetoresistance in the manganates can be understood on the basis of the double-exchange mechanism, but this is too simplistic to account for all the observed data. The most curious property of the manganates relates to the high resistivity exhibited in the so-called metallic state. Charge ordering competes with the double-exchange interaction responsible for ferromagnetism and GMR in these materials. The charge-ordered (charge-crystal) insulating state in the rare earth manganates can be melted into a metallic and ferromagnetic charge-liquid state by applying a magnetic field, thus providing a unique case of charge and spin separation in solids. The observation of GMR in $Tl_2Mn_2O_7$ shows that there can be causes other than double-exchange for the phenomenon.

Keywords: charge ordering · giant magnetoresistance · magnetoresistance · manganates · rare earth manganates

Introduction

Many solids exhibit a change in their resistance on application of a magnetic field. The change in resistance relative to the initial resistance is referred to as magnetoresistance (MR) and is defined by Equation (1), where $\rho(H)$ and $\rho(O)$ are the values of the

$$MR = [\rho(H) - \rho(O)]/\rho(O) \quad (1)$$

resistance or resistivity at a given temperature in the presence and the absence of the magnetic field, respectively. The sign of MR can be positive or negative. Most metals exhibit magnetoresistance of a few percent. Large magnetoresistance, referred to as giant magnetoresistance (GMR), was first observed in bimetallic or multimetallic layers containing ferromagnetic and antiferromagnetic or nonmagnetic metals (e.g. Fe–Cr, Co–Ag) as well as in granular materials[1] wherein the ferromagnetic granules are dispersed in a paramagnetic metal film as in Co/Cu. GMR in these materials arises because the magnetic field changes and controls the scattering of the conduction electrons in the metal by modifying the electron–orbit and spin–orbit interactions. Considerable research has been carried out on the GMR in metallic materials in the last few years because of the vital technological applications in magnetic recording, sensors and the like. The discovery of GMR in rare earth manganates,[2–4] $Ln_{1-x}A_xMnO_3$ (Ln = rare earth, A = divalent ion such as Ca, Sr, Ba or Pb), of the perovskite structure has created excitement, the phenomenon being closely interwoven with the chemistry, electronic structure and magnetic properties of the oxide system.

[*] Prof. Dr. C. N. R. Rao
CSIR Centre of Excellence in Chemistry and
Solid State and Structural Chemistry Unit
Indian Institute of Science, Bangalore - 560 012 (India)
e-mail: cnrrao@sscu.iisc.ernet.in

Discussion

Unique Features of Rare Earth Manganates: Let us examine the nature of rare earth manganates to understand what makes them special. $LaMnO_3$, as the formula dictates, has Mn in the +III state. One can introduce Mn^{4+} ions by aliovalent substitution as in $La_{1-x}Ca_xMnO_3$. When there is a sufficient proportion of Mn^{4+}, the oxide becomes ferromagnetic and concomitantly exhibits metal-like conductivity.[5] Accordingly, the electrical resistivity increases with decrease in temperature like in an insulator until the ferromagnetic Curie temperature, T_c. Below T_c, the resistivity decreases with temperature as in a metal. Thus, an insulator–metal (I–M) transition occurs around T_c as shown in Figure 1. This is understood on the basis of the double-exchange mechanism of Zener[6].

Zener's mechanism involves an electron hopping from Mn^{3+} (d^4, $t_{2g}^3e_g^1$, $S = 2$) to Mn^{4+} (d^3, t_{2g}^3, $S = 3/2$) *via* the oxide ion so that Mn^{3+} and Mn^{4+} ions exchange places [Eq. (2)]. This in-

$$Mn^{3+}O^{2-}Mn^{4+} \longrightarrow Mn^{4+}O^{2-}Mn^{3+} \quad (2)$$

volves the transfer of an electron from the Mn^{3+} site to the central oxide ion and simultaneously the transfer of an electron from the oxide ion to the Mn^{4+} site. Such a transfer is referred to as *double-exchange*. The integral defining the exchange energy in such a system is nonvanishing only if the spins of the two d shells are parallel. That is, the lowest energy of the system is one with a parallel alignment of the spins on the Mn^{3+} and Mn^{4+} ions. This is indeed a novel situation where the lining up of the spins of the incomplete d orbitals of the adjacent Mn ions

  0947-6539/96/0212-1499 $ 15.00+.25/0

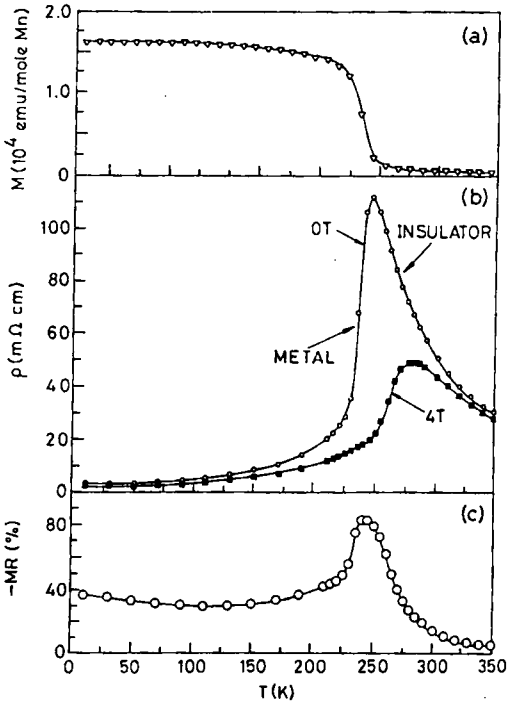

Fig. 1. Variation with temperature of a) the magnetization, b) electrical resistivity (in the absence and presence of a magnetic field) and c) magnetoresistance, MR, in $La_{0.75}Ca_{0.25}MnO_3$ (adapted from ref. [9]). Magnetic field strength is given in tesla (T).

is accompanied by an increase in the rate of hopping of electrons and therefore by an increase in electrical conductivity. Thus, the mechanism that leads to enhanced electrical conductivity requires a ferromagnetic coupling. It is assumed here that the intraatomic exchange, J, is large compared to the transfer integral, t_{ij}, between the two Mn sites.

The relation between the electrical conductivity and ferromagnetism by the double-exchange mechanism is readily obtained. The magnitude of the exchange energy, ε, is given by Equation (3), where is v the frequency of oscillation of

$$\varepsilon = hv/2 \quad (3)$$

the electron between two Mn sites. The diffusion coefficient for an Mn^{4+} ion is defined by Equation (4), where a is the

$$D = a^2\varepsilon/h \quad (4)$$

lattice parameter. Making use of the Einstein equation relating conductivity (σ) and D, $\sigma = ne^2D/kT$, where n is the number of Mn^{4+} ions per unit volume, we obtain Equation (5).

$$\sigma = xe^2\varepsilon/ahkT \quad (5)$$

Here x is the fraction of Mn^{4+} ions in $La_{1-x}A_xMnO_3$. Since the ferromagnetic Curie temperature T_c is related to the exchange energy by the approximate relation, $\varepsilon \approx kT_c$, Equation (6) relates the electrical conductivity to ferromagnetic

$$\sigma \approx (xe^2/ah)(T_c/T) \quad (6)$$

T_c and the fraction of Mn^{4+} ions. We would therefore expect the I–M transition in the manganates to occur at T_c. Double-exchange is strongly affected by structural parameters such as the Mn-O-Mn angle or the Mn–Mn transfer integral.

The double-exchange discussed above is different from superexchange, which also describes cation–anion–cation interactions. The Anderson–Goodenough–Kanamori rules[7] apply to superexchange. According to these rules, a 180° interaction in a d^3–oxygen–d^3 system is antiferromagnetic, but a d^3–oxygen–d^4 interaction would be ferromagnetic. This interaction would not, however, give rise to increased electrical conduction as in the double-exchange mechanism. Zener's model has been extended or modified by several workers. In particular, de Gennes has shown that the energy of the electrons is lowered if there is canting of the sublattices, giving rise to a canted-spin antiferromagnetic state, a situation found when x in $Ln_{1-x}A_xMnO_3$ is small.[8]

The t_{2g}^3 electrons of Mn^{3+} are localized on the Mn site, but the e_g orbital is hybridized with the oxygen 2p orbitals. The e_g state can be localized or itinerant and there is strong coupling between the t_{2g} and e_g electrons. Because Mn^{3+} is a Jahn–Teller ion, we would expect certain structural distortions in the manganates. Accordingly, the crystal structure of stoichiometric $LaMnO_3$ is orthorhombic ($b > a > c^{1/2}$) with three Mn–O distances (1.91, 1.96, 2.19 Å) due to Jahn–Teller distortion. The structure becomes rhombohedral or pseudocubic on progressive substitution of La by divalent cations. Larger A-site cations favour the rhombohedral structure and increase the width of the e_g band. Itinerant e_g electrons resulting from double-exchange would be expected to minimize the effects due to the Jahn–Teller distortion.

In $La_{1-x}Ca_xMnO_3$, both the end members $LaMnO_3$ and $CaMnO_3$ are antiferromagnetic with A- and G-type ordering, respectively. Ferromagnetism is found when in the composition range $x = 0.1$–0.5. When $x > 0.5$, the material is antiferromagnetic. In Figure 2 we show the phase diagram of the

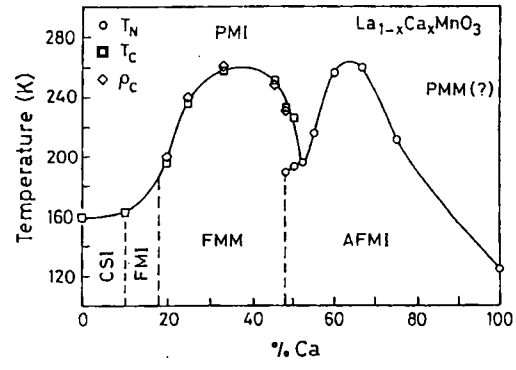

Fig. 2. Temperature–composition diagram of $La_{1-x}Ca_xMnO_3$: CSI, canted-spin insulator; FMI, ferromagnetic insulator; FMM, ferromagnetic metal; AFMI, antiferromagnetic insulator; PMI, paramagnetic insulator; PMM, paramagnetic metal (adapted from ref. [9]). There could be polaron ordering when $x \approx 0.1$.

$La_{1-x}Ca_xMnO_3$ system[9] to illustrate how the electronic and magnetic properties vary with the composition. The nature of the phase diagram varies with the Ln and the divalent cations in $Ln_{1-x}A_xMnO_3$, since the average size of the A-site cations (Ln, A) in these perovskites has a marked effect on the electronic structure. For example, the size of the A-site cations determines the Mn-O-Mn angle and the nature of the e_g electron.

We have hitherto considered manganates of the type $Ln_{1-x}A_xMnO_3$ where the divalent A ions introduce Mn^{4+} ions. Mn^{4+} ions can also be created by chemical or electrochemical means.[10] It is thus possible to prepare $LaMnO_3$ with 33% Mn^{4+}. The structure of $LaMnO_3$ changes to rhombohedral or pseudocubic on increasing the Mn^{4+} content and the material becomes ferromagnetic.[10, 11] Around T_c, an insulator–metal transition occurs just as in $La_{1-x}Ca_xMnO_3$ (Fig. 3). The Mn^{4+}

0947-6539/96/0212-1500 $ 15.00+.25/0 Chem. Eur. J. 1996, 2, No. 12

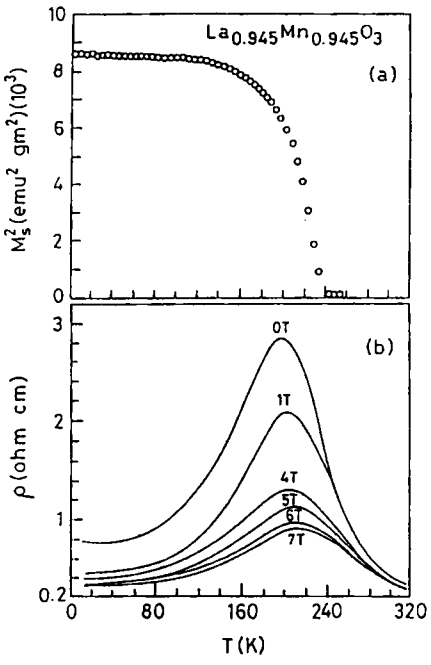

Fig. 3. Variation with temperature of a) the magnetization and b) the resistivity of $La_{0.945}Mn_{0.945}O_3$ in presence and absence of magnetic field (adapted from ref. [11]).

ions are created in $LaMnO_3$ by the presence of cation vacancies in the La and Mn sites to nearly an equal extent, and not by oxygen excess.[12] $LaMnO_3$ with 33% Mn^{4+} is therefore described as $La_{0.945}Mn_{0.945}O_3$. One can prepare samples with a greater proportion of vacancies in the La or the Mn site. The latter destroys ferromagnetism and the I–M transition if the vacancy concentration is greater than 5%.

Magnetotransport Properties and GMR: From Figures 1 and 3, we see that the manganates undergo an insulator–metal (I–M) transition in the vicinity of the ferromagnetic Curie temperature, T_c. Usually, the I–M transition occurs at a temperature, T_{IM}, slightly lower than T_c. Application of a magnetic field drastically reduces the resistivity, especially in the T_c region. Transport properties and GMR of a large number of $Ln_{1-x}A_xMnO_3$ derivatives have been investigated in the last three years, with samples in the polycrystalline pellet,[11, 13–15] thin film[3, 16–18] or single crystal forms.[4, 19] These studies have revealed certain general features, which are summarized below:

1) Around 30% Mn^{4+} is optimal to observe ferromagnetism and GMR in the manganates.
2) The magnitude of GMR is generally high and can reach up to 100%, especially in the T_c region. Some workers report very high values of GMR, because they use $\rho(H)$ in the denominator of Equation (1) or give $\rho(O)/\rho(H)$ ratios.
3) High resistivity at the I–M transition and low T_c favour GMR.[11] Magnetoresistance is found to scale with the field-induced magnetization, that is, MR = $C(M/M_s)^2$ where M_s is the saturation magnetization and C is a constant.[4]
4) The T_c increases with hydrostatic pressure because of the change in the Mn-O-Mn angle or the Mn–Mn transfer integral.[20] Increasing the radius of the A-site cation, $\langle r_A \rangle$, has the same effect as the hydrostatic pressure.[13, 20, 21] A plot of T_c against $\langle r_A \rangle$ or pressure gives a phase diagram that separates the ferromagnetic metal and the paramagnetic insulator regimes (Fig. 4).[15]

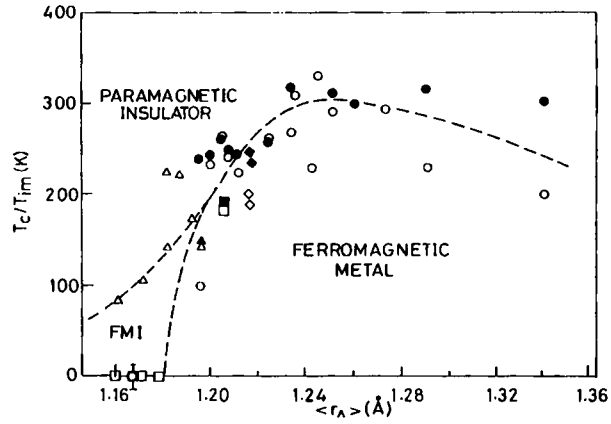

Fig. 4. Variation of T_c and the temperature of the insulator–metal transition, T_{IM}, with average size of the A-site cation, $\langle r_A \rangle$, in rare earth manganates (adapted from ref. [15]). FMI, ferromagnetic insulator.

5) Dimensionality affects the magnitude of GMR.[22] In the $(SrO)(La_{1-x}Sr_xMnO_3)_n$ system, the $n = 2$ member shows a sharp I–M transition and the highest MR. The $n = 2$ member has a dimensionality between 2 and 3, since the $n = 1$ member has the two-dimensional K_2NiF_4 structure and the $n = \infty$ member is the three-dimensional perovskite. This is probably due to a competition between the in-plane antiferromagnetic interaction and the double-exchange interaction.
6) Particle size has negligible effect on MR, although long-range ferromagnetic order is adversely affected.[23] Nanometric particles of the manganates show GMR, although they do not exhibit a sharp ferromagnetic transition. It would appear as though the presence of small domains or Mn^{3+}-O-Mn^{4+} clusters is sufficient for GMR to be observed. Large differences between T_{IM} and T_c also occur in samples of different particle sizes prepared at different temperatures.
7) The manganates exhibiting GMR generally have unusually high resistivities not only in the insulating regime, but even in the so-called metallic regime. Thus, resistivities of some of these materials are very high at low temperatures, reaching values of $\approx 10^4$ Ωcm. The values of resistivity in the metallic regime are very much higher than the maximum metallic resistivity defined by Mott.[24] Accordingly, the manganates possess a negligible density of states at the Fermi level even in the metallic state. The photoelectron spectra of $Ln_{1-x}Sr_xMnO_3$ compositions shown in Figure 5 demonstrate this feature.[25, 26] The insulating compositions have still lower density of states than the metallic compositions.[27]

Charge versus Spin Ordering: The study of GMR in the rare earth manganates has unravelled unique features related to the charge and spin dynamics in these oxides. Charge ordering in metal oxides is not a new phenomenon. Fe_3O_4 (magnetite) undergoes the Verwey transition at around 120 K due to charge ordering accompanied by a resistivity anomaly. Charge ordering is observed in the manganates when the Mn^{3+} and Mn^{4+} populations are roughly comparable. Double-exchange gives rise to a metallic, ferromagnetic state, while the charge-ordered state is generally insulating and antiferromagnetic. This is understandable since electrons become localized when the Mn^{3+} and Mn^{4+} ions become ordered; only when electrons hop from site to site, does the material become ferromagnetic owing to double-exchange. The charge-ordered state can be melted into a

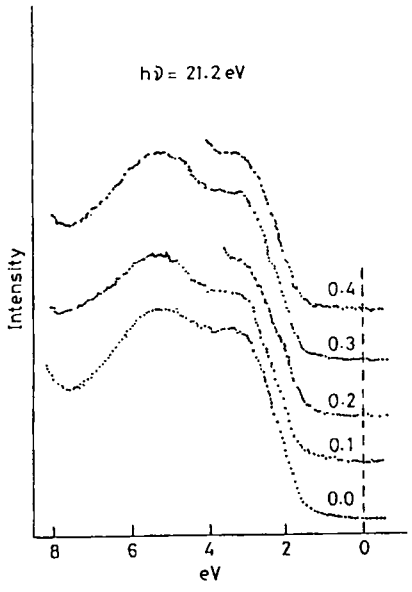

Fig. 5. Photoelectron spectra of $La_{1-x}Sr_xMnO_3$ in the valence-band regime (from ref. [25]).

metallic spin-ordered (ferromagnetic) state, by the application of a magnetic field. Such a separation of charge and spin in the manganates is indeed noteworthy.

There are essentially two scenarios of charge ordering in the manganates. These are typified by $Nd_{0.5}Sr_{0.5}MnO_3$ and $Pr_{0.7}Ca_{0.3}MnO_3$. $Nd_{0.5}Sr_{0.5}MnO_3$ is a ferromagnetic metal at 250 K and becomes an antiferromagnetic insulator on cooling to 150 K, owing to charge ordering, accompanied by changes in lattice parameters (Fig. 6).[28] $Pr_{0.7}Ca_{0.3}MnO_3$, on the other hand, is in the charge-ordered insulating state at 200 K, and becomes antiferromagnetic at 140 K and transforms to a canted-spin antiferromagnetic state at 110 K.[29] This oxide does not exhibit the metallic ferromagnetic state at any temperature. We present these scenarios schematically in Figure 7.

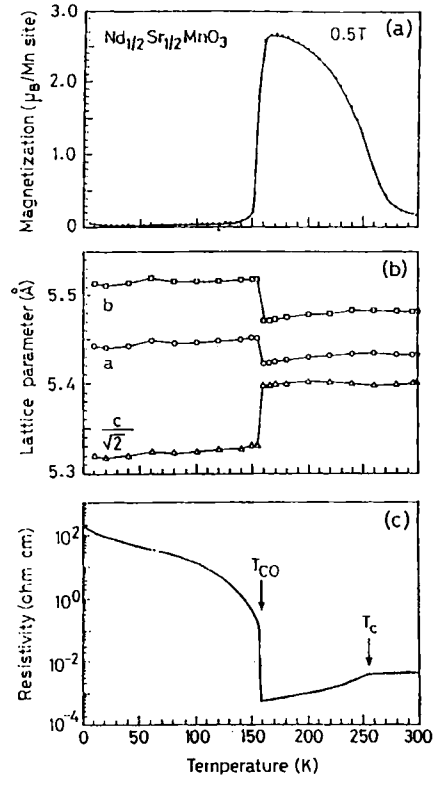

Fig. 6. The variation of a) magnetization, b) lattice parameters and c) electrical resistivity of $Nd_{0.5}Sr_{0.5}MnO_3$ with temperature (from ref. [28]).

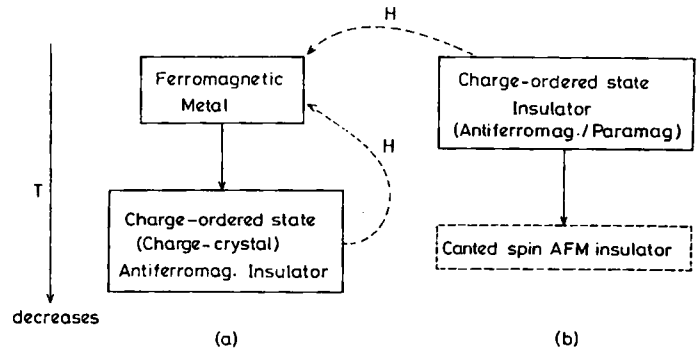

Fig. 7. Schematic presentation of two typical scenarios of charge ordering in rare earth manganates. Dotted arrows show how, by the application of a magnetic field, H, the charge-ordered state can be melted into a ferromagnetic and metallic (charge-liquid) state. Scenario (a) is found in $Nd_{0.5}Sr_{0.5}MnO_3$ and (b) in $Pr_{0.7}Ca_{0.3}MnO_3$.

Charge ordering in the manganates is governed by the width of the e_g band, which is determined by the weighted average radius of the A-site cations, $\langle r_A \rangle$, or the tolerance factor. This is because a distortion in the Mn-O-Mn bond angle affects the transfer interaction of the e_g conduction electrons. The spin and charge-ordering phenomena in the rare-earth manganates can be described in terms of the generalized phase diagram in Figure 8. The diagram shows that when $\langle r_A \rangle$ is large (e.g., $La_{1-x}Sr_xMnO_3$), ferromagnetism and the associated I–M transition are found, but charge ordering is not observed. With decreasing $\langle r_A \rangle$, we observe a ferromagnetic state, which transforms to the antiferromagnetic charge-ordered state on cooling (e.g., $Nd_{0.5}Sr_{0.5}MnO_3$). When $\langle r_A \rangle$ is very small as in $Pr_{0.7}Ca_{0.3}MnO_3$ and $Nd_{0.5}Ca_{0.5}MnO_3$, no ferromagnetism occurs, but there is a charge-ordered state; the ferromagnetic metallic state is created only by the application of a magnetic field to the charge-ordered state. We compare the magnetic and electronic phase diagrams of $Pr_{1-x}Sr_xMnO_3$ and $Pr_{1-x}Ca_xMnO_3$[31] in Figure 9 to illustrate the effect of the e_g

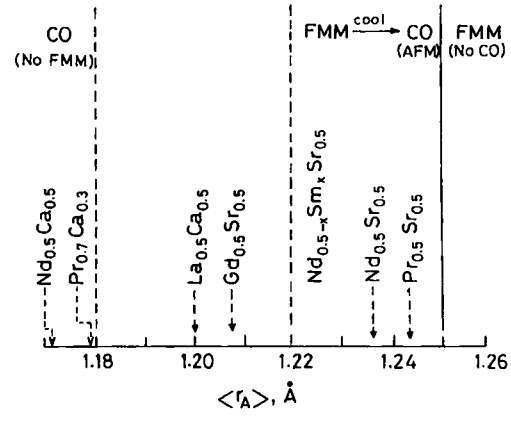

Fig. 8. Schematic phase diagram showing the prevalence of charge-ordered (CO) and ferromagnetic (FMM) states in $Ln_{1-x}A_xMnO_3$ depending on the average radius of the A-site cation, $\langle r_A \rangle$ (AFM, antiferromagnetic).

0947-6539/96/0212-1502 $ 15.00+.25/0 Chem. Eur. J. 1996, 2, No. 12

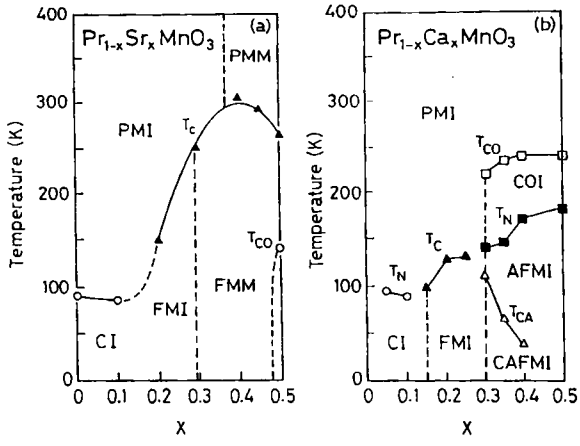

Fig. 9. The magnetic and electronic phase diagrams of $Pr_{1-x}Sr_xMnO_3$ and $Pr_{1-x}Ca_xMnO_3$ (adapted from ref. [31]). CI, canted spin insulator; COI, charge-ordered insulator; CAFMI, canted antiferromagnetic insulator (for further abbreviations see legend to Fig. 2).

bandwidth. A recent study[30] of $Nd_{0.5}Ca_{0.5}MnO_3$ has shown a first-order transition at around 200 K with a large change in volume due to charge ordering accompanied by changes in the bond angles and bond lengths (Fig. 10) in the *ab* plane. Such

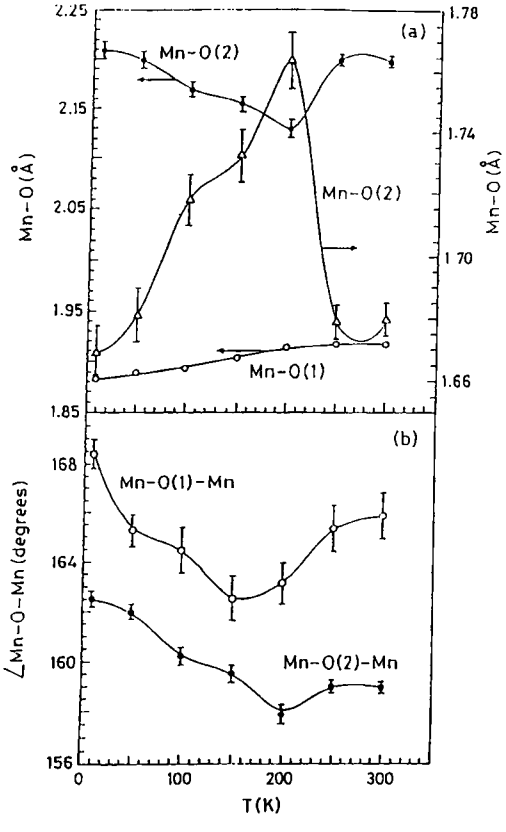

Fig. 10. Variation of Mn–O distances and Mn-O-Mn angles due to charge ordering in $Nd_{0.5}Ca_{0.5}MnO_3$ (from ref. [30]).

large changes in structural parameters would be expected to occur due to charge ordering.

The charge-ordered insulating state (charge-crystal state) can be melted into a charge-liquid (metallic) state which is ferromagnetic by the application of a magnetic field (see Fig. 7). In Figure 11 we show this phenomenon in the case of $Pr_{0.7}Ca_{0.3}MnO_3$.[29] Such resistivity transitions induced by magnetic fields are thermodynamically first order and exhibit considerable hysteresis effects.[28, 31] The electronic phase diagrams of two typical manganates in the temperature–magnetic field plane[31] are shown in Figure 12 to demonstrate how the field-induced metallic regime is sensitive to the size of the A-site cations. Collapse of the charge-ordered state to a metallic state in a magnetic field is related to GMR, which is a field-induced change in resistivity.

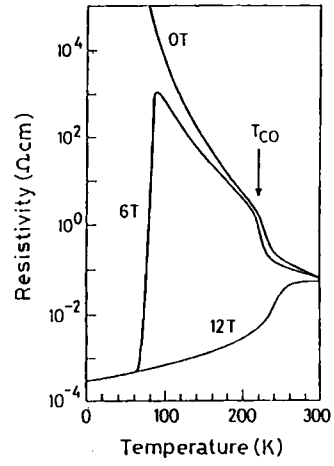

Fig. 11. Temperature variation of resistivity of $Pr_{0.7}Ca_{0.3}MnO_3$ in the presence and absence of magnetic field (adapted from ref. [29]).

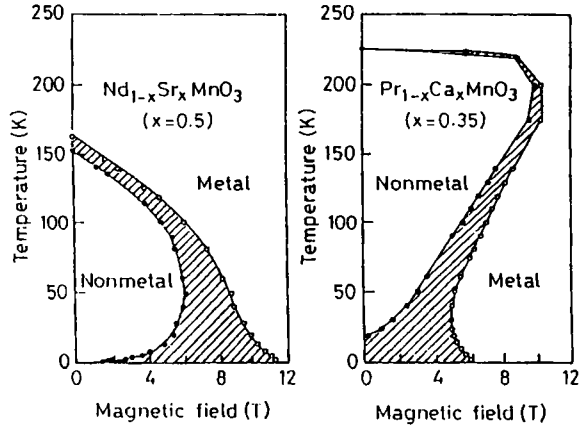

Fig. 12. Electronic phase diagrams of $Nd_{0.5}Sr_{0.5}MnO_3$ and $Pr_{0.65}Ca_{0.35}MnO_3$ in the T–H plane (adapted from ref. [31]).

$Tl_2Mn_2O_7$ and $La_{1-x}A_xCoO_3$: $Tl_2Mn_2O_7$ with the pyrochlore structure also exhibits GMR although it primarily contains Mn^{4+} ions.[32] This oxide undergoes a transition from a paramagnetic metallic phase to a ferromagnetic metallic phase ($T_c \approx 140$ K). The Mn–O distance is around 1.90 Å, and electrons are the charge carriers, unlike in $Ln_{1-x}A_xMnO_3$ where holes are the charge carriers. The resistivity is quite low from 300 K down to low temperatures. GMR in $Tl_2Mn_2O_7$ seems to have a different origin, since double-exchange cannot occur as in the rare earth manganates. $La_{1-x}A_xCoO_3$ (A = Ca, Sr, Ba), which becomes ferromagnetic and metallic above a value of $x = 0.15$, shows GMR in the insulating phase at low temperatures.[33]

Concluding Remarks

Giant magnetoresistance in rare earth manganates is clearly linked to the ferromagnetism and the insulator–metal transition arising from the double-exchange mechanism. Based on double-exchange, one can understand the gross behaviour of materials such as $La_{1-x}Sr_xMnO_3$ which have relatively broad e_g bands.[34] According to such a simple model, GMR arises from the strong spin–charge coupling (Hund's coupling) between the t_{2g} and e_g electrons. Application of a magnetic field causes a

reduction in the spin-disorder scattering of the e_g electrons. The double-exchange model, however, cannot explain all the observations, especially the anomalous resistivity of the manganates. In order to understand the resistivity behaviour across the insulator–metal transition, especially in narrow-band materials involving small A-site cations, it is necessary to invoke electron–lattice coupling.[35, 36] Millis et al.[35] propose that electron–phonon interaction arising from the Jahn–Teller splitting of the Mn d levels plays a crucial role. Jahn–Teller distortions localize conduction electrons as polarons. As the temperature decreases, the transfer integral t_{ij} increases and the ratio of the Jahn–Teller energy to t_{ij} decreases. The coupling can vary with temperature and composition. The coupling would increase across the metal–insulator transition. The large oxygen isotope effect on T_c recently observed also suggests that the coupling of the charge carriers to the lattice is important.[37] Electron–lattice interaction alone cannot, however, explain the high resistivities of the materials, particularly at low temperatures. On-site Coulomb correlations together with antiferromagnetic exchange interactions involving the t_{2g} states could also be important.[38] Coey et al.[39] argue that when $T < T_c$, the e_g electrons are delocalized on an atomic scale but the spatial fluctuations in the coulomb- and spin-dependent potentials tend to localize the e_g electrons in wave packets longer than the Mn–Mn distance. Clearly, there is a need to develop models that can explain a variety of unusual properties of the manganates such as charge ordering and the high resistivity of the metallic phase besides the GMR behaviour. As we have seen earlier, there is competition between charge ordering and double-exchange interactions. In order to describe the electrons in the marginally metallic rare earth manganates, it would be necessary not only to incorporate correlation and disorder effects, but also electron–lattice interactions, magnetic polaron effects, etc.[40]

The observation of GMR in $Tl_2Mn_2O_7$ shows that double-exchange alone cannot be responsible for this phenomenon[32]. While exploring for newer systems, this has to be kept in mind, and also that other oxides[33] may exhibit GMR. While magnetoresistance close to 100% has been observed in many of the manganates, the magnetic fields employed are high or the temperature at which GMR occurs is below laboratory temperatures. For a viable use of these materials for technological applications, GMR should occur at room temperature on the application of small fields (1000 G or less). If such materials are found, they will affect a multibillion dollar industry. Clearly, there is scope to explore other oxide systems which may show such properties.

Acknowledgement: The author thanks the Science Office of the European Union and the Department of Science and Technology for support of GMR research.

Received: July 23, 1996 [C418]

[1] P. M. Levy, S. Zhang, *J. Magn. Magn. Mater.* **1995**, *151*, 315.
[2] K. Chahara, T. Ohno, M. Kasai, Y. Kozono, *Appl. Phys. Lett.* **1993**, *63*. 1990.
[3] a) R. Von Helmolt, B. Holzapfel, L. Schultz, K. Samwer, *Phys. Rev. Lett.* **1993**, *71*, 2331. b) M. McCormack, S. Jin, T. Tiefel, R. M. Fleming, J. M. Phillips, R. Ramesh, *Appl. Phys. Lett.* **1993**, *63*, 1990. c) R. Mahesh, R. Mahendiran, A. K. Raychaudhuri, C. N. R. Rao, *J. Solid State Chem.* **1995**, *114*, 297. d) C. N. R. Rao, A. K. Cheetham, *Science* **1996**, *272*, 369.
[4] A. Urishibara, Y. Morimoto, T. Arima, A. Asamitsu, G. Kido, Y. Tokura, *Phys. Rev.* **1995**, *B51*, 14103.
[5] a) G. H. Jonker, J. H. Van Santen, *Physica*, **1950**, *16*, 377. b) J. H. Van Santen, G. H. Jonker, *ibid.* **1950**, *16*, 599.
[6] C. Zener, *Phys. Rev.* **1951**, *82*, 403.
[7] a) P. W. Anderson, H. Hasegawa, *Phys. Rev.* **1955**, *100*, 675. b) J. B. Goodenough, *ibid.* **1955**, 100, 564. c) J. Kanamori, *J. Phys. Chem. Solids*, **1959**, *10*, 87.
[8] P. G. de Gennes, *Phys. Rev.* **1960**, *118*, 141
[9] P. Schiffer, A. P. Ramirez, W. Bao, S. W. Cheong, *Phys. Rev. Lett.* **1995**, *75*, 3336.
[10] a) M. Verelst, N. Rangavittal, C. N. R. Rao, A. Rousset, *J. Solid State Chem.* **1993**, *104*, 74. b) R. Mahesh, K. R. Kannan, C. N. R. Rao, *ibid.* **1995**, *114*, 294.
[11] R. Mahendiran, R. Mahesh, N. Rangavittal, S. K. Tewari, A. K. Raychaudhuri, T. V. Ramakrishnan, C. N. R. Rao, *Phys. Rev.* **1996**, *B56*, 3348.
[12] a) J. A. M. Van Roosmalen, E. H. M. Cordfunke, R. B. Helmholdt, H. W. Zandbergen, *J. Solid State Chem.* **1994**, *110*, 100, 109. b) H. Hervieu, R. Mahesh, N. Rangavittal, C. N. R. Rao, *Eur. J. Solid State Inorg. Chem.* **1995**, *32*, 79.
[13] a) B. Raveau, A. Maignan, V. Caignaert, *J. Solid State Chem.* **1995**, *117*, 424. b) V. Caignaert, A. Maignan, B. Raveau, *Solid State Commun.* **1995**, *95*, 357.
[14] a) R. Mahendiran, R. Mahesh, A. K. Raychaudhuri, C. N. R. Rao, *J. Phys. D.* **1995** *28*, 1743. b) R. Mahendiran, R. Mahesh, A. K. Raychaudhuri, C. N. R. Rao, *Phys. Rev.* **1996**, *B53*, 12160. c) S. Jin, H. M. O'Bryan, T. H. Tiefel, M. McCormack, W. W. Rhodes, *Appl. Phys. Lett.* **1995**, *66*, 180.
[15] R. Mahesh, R. Mahendiran, A. K. Raychaudhuri, C. N. R. Rao, *J. Solid State Chem.* **1995**, *120*, 204.
[16] a) S. Jin, M. McCormack, T. H. Tiefel, R. Ramesh, *J. Appl. Phys.* **1994**, *76*, 6929. b) H. L. Ju, C. Kwon, Q. Li, R. L. Greene, T. Venkatesan, *Appl. Phys. Lett.* **1994**, *65*, 2108. c) J. F. Lawler, J. M. D. Coey, *J. Magn. Magn. Mater.* **1995**, *140–144*, 2049.
[17] a) M. F. Hundley, *Phys. Rev. Lett.* **1995**, *75*, 860. b) G. Q. Gong, C. Canedy, G. Xiao, J. G. Sun, A. Gupta, W. J. Gallagher, *Appl. Phys. Lett.* **1995**, *67*, 1783. c) G. C. Xiong, Q. Li, H. L. Ju, S. N. Mao, L. Senapati, X. X. Xi, R. L. Greene, K. Venkatesan, *ibid.* **1995**, *66*, 1689.
[18] A. Gupta, T. R. McGuire, P. R. Duncombe, M. Rupp, J. Z. Sun, W. J. Gallagher, G. Xiao, *Appl. Phys. Lett.* **1995**, *67*, 3494.
[19] A. Anane, C. Dupas, K. L. Dang, J. P. Renard, P. Veillet, A. M. D. Guevara, F. Millot, L. Pinsard, A. Revcolevschi, *J. Phys. Condens. Matter*, **1995**, *7*, 7015.
[20] a) J. J. Neumeier, M. F. Hundley, J. D. Thompson, R. H. Heffner, *Phys. Rev.* **1995**, *B52*, 7006. b) H. Y. Hwang, T. T. M. Palstra, S. W. Cheong, B. Batlogg, *ibid.* **1995**, *B52*, 15046.
[21] H. Y. Hwang, S. W. Cheong, P. G. Radaelli, M. Mauzio, B. Batlogg, *Phys. Rev. Lett.* **1995**, *75*, 914.
[22] a) R. Mahesh, R. Mahendiran, A. K. Raychaudhuri, C. N. R. Rao, *J. Solid State Chem.* **1996**, *122*, 448. b) Y. Moritomo, A. Asamitsu, H. Kuwahara, Y. Tokura, *Nature* **1996**, *380*, 141.
[23] a) R. Mahesh, R. Mahendiran, A. K. Raychaudhuri, C. N. R. Rao, *Appl. Phys. Lett.* **1996**, *68*, 2291. b) R. Mahendiran, R. Mahesh, A. K. Raychaudhuri, C. N. R. Rao, *Solid State Commun.* **1996**, *99*, 149
[24] According to Mott, there is a minimum metallic conductivity or maximum metallic resistivity at which the material may still be viewed as being metallic, prior to it becoming an insulator, owing to disorder-induced localization of electrons (see N. F. Mott, *Philos. Mag.* **1972**, *26*, 1015).
[25] D. D. Sarma in *Metal–Insulator Transitions Revisited* (Eds.: P. P. Edwards and C. N. R. Rao), Taylor and Francis, London, **1995**.
[26] D. D. Sarma, N. Shanthi, S. R. K. Kumar, T. Saitoh, T. Mizokawa, A. Sekiyama, K. Kobayashi, A. Fujimori, G. Weschcke, R. Meier, G. Kaindl, Y. Takeda, M. Takano, *Phys. Rev.* **1996**, *B53*, 6873.
[27] J. H. Park, C. T. Chen, S. W. Cheong, W. Bao, G. Meigs, V. Chakarian, Y. U. Idzerda, *J. Appl. Phys.* **1996**, *79*, 4558.
[28] H. Kuwahara, Y. Tomioka, A. Asamitsu, Y. Moritomo, Y. Tokura, *Science* **1995**, *270*, 961.
[29] Y. Tomioka, A. Asamitsu, H. Kuwahara, Y. Moritomo, Y. Tokura, *Phys. Rev.* **1996**, *B53*, 1689.
[30] T. Vogt, A. K. Cheetham, R. Mahendiran, A. K. Raychaudhuri, R. Mahesh, C. N. R. Rao, *Phys. Rev. B*, in print.
[31] Y. Tokura, Y. Tomioka, H. Kuwahara, A. Asamitsu, Y. Moritomo, M. Kasai, *J. Appl. Phys.* **1996**, *79*, 5288.
[32] a) Y. Shimakawa, Y. Kubo, T. Manako, *Nature* **1996**, *379*, 53. b) M. A. Subramanian, B. H. Toby, A. P. Ramirez, W. J. Marshall, A. W. Slieght, G. H. Kwei, *Science* **1996**, *273*, 81
[33] G. Briceno, H. Chang, X. Sun, P. G. Schultz, X. D. Xiang, *Science* **1995**, *270*, 273
[34] N. Furakawa, *J. Phys. Soc. Jpn.* **1994**, *63*, 3214.
[35] A. J. Millis, P. B. Littlewood, B. I. Shraiman, *Phys. Rev. Lett.* **1995**, *74*, 5144.
[36] H. Röder, J. Zang, A. R. Bishop, *Phys. Rev. Lett.* **1996**, *76*, 1356.
[37] G. Zhao, K. Conder, H. Keller, K. A. Muller, *Nature* **1996**, *381*, 676.
[38] J. Inoue, S. Maekawa, *Phys. Rev. Lett.* **1995**, *74*, 3407.
[39] J. M. D. Coey, M. Viret, L. Ranno, K. Ounadjeda, *Phys. Rev. Lett.* **1995**, *75*, 3910.
[40] C. N. R. Rao, *Chem. Commun.* **1996**, 2217.